Proceeding Series of the Brazilian Society of Computational and Applied Mathematics, v. 12, n. 1, 2026.

Trabalho apresentado no XLIV CNMAC, Fundação Getulio Vargas - Rio de Janeiro - RJ, 2025.

Proceeding Series of the Brazilian Society of Computational and Applied Mathematics

Modeling Nanoparticle-Stabilized Foam Flow in Porous Media: Mathematical Analysis and Uncertainty Quantification

Tatiana D. Assis[1], Grigori Chapiro[2]
UFJF, Juiz de Fora, MG

Abstract. Foam injection with nanoparticles can be useful in various subsurface applications, particularly in challenging field conditions such as oil production in the Brazilian Pre-Salt. By enhancing foam stabilization, nanoparticles improve their effectiveness as mobility-control agents in gas flooding. We propose new models of nanoparticle-stabilized foam flow in porous media, accounting for nanoparticle transport and its effect on reducing foam mobility. The first model considers foam at local equilibrium and is governed by a non-strictly hyperbolic system of conservation laws. The existence and uniqueness of a global solution as a sequence of waves are proved using entropy conditions. The analytical solution is utilized to evaluate the impact of nanoparticles on key industrial parameters such as breakthrough time, water production, and pressure drop over time. We also perform sensitivity analysis and uncertainty quantification studies. The second and more complex model accounts for particle retention and permeability reduction. In this case, a steady-state semi-analytical solution is presented. It is then used to investigate the impact of nanoparticle retention on water saturation, foam's apparent viscosity, and pressure drop profiles. We also discuss two opposing effects of retention on pressure drop and how models that neglect one or both of these effects underestimate pressure.

Keywords. Nanoparticle-Stabilized Foam, Flow in Porous Media, Particle Retention, Uncertainty Quantification, Sensitivity Analysis.

1 Introduction

Nanotechnology has rapidly advanced in various industrial sectors, particularly in subsurface applications such as soil and aquifer remediation, CO_2 storage, and enhanced oil recovery [12]. One promising application of nanoparticles is in stabilizing emulsions and foams, which serve as mobility-control agents to optimize gas flooding [7]. There is significant interest in applying foam injection in the Brazilian Pre-Salt, where water alternating gas (WAG) injection is commonly used. The heterogeneous nature of this carbonate reservoir, combined with the need to re-inject the produced CO_2, leads to issues such as high viscous fingering, channeling, and gravity override, all of which reduce sweep efficiency [9]. While foam can help mitigate these phenomena, ensuring its long-term stability remains challenging, particularly in the presence of salt, brine, and high temperatures. As a result, nanoparticle-stabilized foam may represent the next step in improving oil production in challenging fields like the Pre-Salt. Although experiments [16] have shown that adding nanoparticles improves foam stability and resistance, particle retention is a significant concern, as it can reduce rock permeability and lead to injectivity loss in injection wells [8]. For

[1]tatiana.danelon@ufjf.br
[2]grigori.chapiro@ufjf.br

foam assisted by nanoparticles (NP-stabilized foam), retention can also limit available particles for stabilization, reducing foam flow efficiency.

Modeling foam flow in porous media is a well-researched area [17], but incorporating nanoparticles is quite complex. Two studies [6, 7] have provided numerical solutions for foam models calibrated with NP-stabilized foam experimental data. Another study [13] introduced nanoparticle concentration as a variable, though its solution was also numerical. This work provides a summary of my PhD thesis [2] by reviewing three papers [3–5] that introduce two NP-stabilized foam models allowing for analytical investigations. Both models are based on the Stochastic Bubble Population Balance model [17]. One model assumes foam at local equilibrium and neglects retention, while the other is a population balance model that takes retention into account.

Since mathematical models are calibrated using laboratory experimental data, it is crucial to investigate how input data uncertainties impact model predictions [15]. However, these analyses can be expensive due to the high number of model calls required, especially for complex models [15]. In [5], we conducted uncertainty quantification and sensitivity analysis using an analytical solution for NP-stabilized foam flow, which accelerates calculations and achieves fast convergence.

2 Mathematical Modeling and Analytical Investigation

This study examines one-dimensional water-gas flow in a saturated porous medium in the presence of foam and with nanoparticles in the aqueous phase. We assume a simultaneous flow of gas and a surfactant-nanoparticle solution within a homogeneous rock, with both phases incompressible and immiscible. A large-scale approximation is applied, neglecting diffusion terms. Foam is a non-Newtonian fluid, with its apparent viscosity (μ_{app}) depending on the gas velocity (u_g). Let μ_g be the viscosity of the foam-free gas and d a constant related to the fluid viscosity. Based on [11], we propose

$$\mu_{\text{app}} = \mu_g + \alpha(C) n u_g^d, \tag{1}$$

where $\alpha(C) = \alpha_1 C + \alpha_0$ is a function of suspended nanoparticle concentration (C), incorporating the effect of nanoparticles on foam stabilization by increasing the foam's apparent viscosity.

In [3], the complete model describing NP-stabilized foam flow is a system of five unknowns: water saturation (S_w), suspended (C) and retained (σ) nanoparticle concentration, foam texture (n), and pressure (P, neglecting capillary effects). Based on [8, 17], this system of partial differential equations is given by

$$\varphi \partial_t S_w + U \partial_x f_w = 0, \tag{2}$$
$$U = -k(k_{rw}/\mu_w + k_{rg}/\mu_{\text{app}})\partial_x P, \tag{3}$$
$$\varphi \partial_t [n(1 - S_w)] + U \partial_x [n(1 - f_w)] = \varphi(1 - S_w) K_g (n_\infty - n), \tag{4}$$
$$\varphi \partial_t (C S_w + \sigma) + U \partial_x (C f_w) = 0, \tag{5}$$
$$\partial_t \sigma = \lambda U C f_w. \tag{6}$$

Equations (2) and (3) represent the water mass conservation and Darcy's Law, respectively, where φ is the porosity, k is the absolute permeability, and U is the total superficial velocity. The fractional flow function is $f_w = k_{rw}/[k_{rw} + (\mu_w/\mu_{\text{app}})k_{rg}]$, where k_{rw} and k_{rg} are the relative permeabilities of water and gas, and μ_w is the water viscosity. Equation (4) describes the bubble balance, which is influenced by the bubble generation rate (K_g) and the equilibrium foam texture (n_∞). Equations (5) and (6) represent the transport of nanoparticles in the water phase. Following the Colloid Filtration Theory (CFT) [10], the retained nanoparticle concentration (σ) increases over time depending on a filtration coefficient (λ).

DOI: 10.5540/03.2026.012.01.0313

Consider normalized water saturation $S = (S_w - S_{wc})/(1 - S_{wc})$, where S_{wc} is the connate water and S_{gr} is the residual gas. Following the Corey model, the relative permeabilities for water and gas phases are

$$k_{rw}^0(S) = c_{k_{rw}} S^{n_w}, \quad k_{rg}^0(S) = c_{k_{rg}}(1 - S)^{n_g}, \tag{7}$$

where $c_{k_{rw}}$ and $c_{k_{rg}}$ represent the endpoint relative permeabilities for each phase. The exponents are defined as $n_w = \tau$ and $n_g = (3\tau + 2)/\tau$, with $\tau = 5$ being a parameter related to pore size distribution. The retained nanoparticles decrease the original relative permeabilities as [1]

$$k_{rw}(S_w, \sigma) = \frac{k_{rw}^0(S_w)}{1 + \theta_w \sigma}, \quad k_{rg}(S_w, \sigma) = \frac{k_{rg}^0(S_w)}{1 + \theta_g \sigma}, \tag{8}$$

where θ_w and θ_g are positive constants called permeability-reduction factors.

The system (2)-(6) is quite complex to allow an analytical solution. Therefore, in [3], we studied the steady-state case. The flow velocities u_w and u_g are assumed to be independent of x as follows.

$$u_w = -\frac{k c_{k_{rw}} S^\tau}{\mu_w (1 + \theta_w \sigma)} d_x P, \quad u_g = -\frac{k c_{k_{rg}} (1 - S)^{3 + \frac{2}{\tau}}}{[\mu_g + (\alpha_1 C + \alpha_0) n u_g^d](1 + \theta_g \sigma)} d_x P. \tag{9}$$

At steady-state, the bubble balance equation is also simplified to

$$d_x n = \varphi u_g^{-1} (1 - S_{wc})(1 - S) K_g (n_\infty - n). \tag{10}$$

According to the CFT, the solutions for C and σ are given by [1]: $C(x,t) = C^I e^{-\lambda x}$ and $\sigma(x,t) = \lambda C^I (Ut - \varphi x) e^{-\lambda x}$, for $x < ut/\varphi$ (otherwise, both concentrations C and σ vanish). To find the stationary solution, we used the approximation $\sigma(x) = \Gamma C(x) = \Gamma C^I e^{-\lambda x}$ [3], applicable for a limited time. In the case without nanoparticles, $S(x)$ can be calculated analytically, while for the general case, it is obtained numerically. Foam texture and pressure profiles are derived from the known water saturation profile. For more details, see [3].

In [4], we introduced a simplified version of the system (2)-(6), ignoring particle retention and assuming foam at local equilibrium. It is a non-strictly hyperbolic system described by only two unknowns (S and C). Considering a Riemann problem, we sought a global solution composed of shock, rarefaction, and contact waves, following the principles of Conservation Laws Theory. We proved the existence and uniqueness of the solution by imposing an appropriate entropy condition, which establishes the necessary and sufficient conditions to ensure wave sequence compatibility. By classifying the entire phase-plane S-C, six distinct solution types are identified; see [4] for a detailed construction of each type. The simplified model's sensitivity and uncertainty were further examined in [5] using quadratic Corey exponents ($n_w = n_g = 2$ in equation (7)). We verified that the quadratic model's solution [5] is qualitatively the same as the original model while enabling faster calculations through algebraic expressions for solution profiles. It is worth noting that, when ignoring retention and under steady-state conditions, the dynamic solution of the simplified model is equivalent to the steady-state solution of the complete model; see [3] for such a comparison.

3 Applications

This section examines applications of the mathematical models discussed in Section 2 concerning NP-stabilized foam flow. The physical parameters are based on core-flood experiments involving SDS surfactant and silica (SiO_2) nanoparticles [6, 14]; see Table 1.

Table 1: Model parameters used in this work. Source: [6, 14].

Parameter	Value	Parameter	Value	Parameter	Value
α_0 (Pa $\mathrm{s}^{\frac{2}{3}}\mathrm{m}^{\frac{10}{3}}$)	$5.8 \cdot 10^{-16}$	$c_{k_{rg}}$ $(-)$	1.0	L (m)	0.17
α_1 (Pa $\mathrm{s}^{\frac{2}{3}}\mathrm{m}^{\frac{10}{3}}$)	$1.83 \cdot 10^{-15}$	$c_{k_{rw}}$ $(-)$	0.75	D (m)	0.038
μ_g (Pa s)	$1.8 \cdot 10^{-5}$	u_w (m/s)	$1.45 \cdot 10^{-6}$	K_g (s^{-1})	0.10
μ_w (Pa s)	$1.0 \cdot 10^{-3}$	u_g (m/s)	$1.47 \cdot 10^{-5}$	n_∞ (mm^{-3})	802.58
ϕ $(-)$	0.21	S_{wc} $(-)$	0.10		
k (m^2)	$2.5 \cdot 10^{-12}$	S_{gr} $(-)$	0		

3.1 Effect of Nanoparticles on Foam Flow Neglecting Retention

In [4], we studied NP-stabilized foam flow at local equilibrium and neglecting retention. We consider a Riemann problem with left state $(S, C)(x, 0) = (S_L, C_L)$ if $x < 0$ (injection condition) and right state $(S, C)(x, 0) = (S_R, C_R)$ if $x \geq 0$ (initial reservoir condition). This paper [4] focuses on the drainage procedure after a slug of water with surfactant and nanoparticles. That is the region where the gas bank (low S_L, $C_L = 0$) meets the slug (high S_R, $C_R \geq 0$). It was found that when only gas is injected, both the breakthrough time and water production increase with the concentration of nanoparticles. However, this effect is less significant at higher concentrations.

The left panel in Figure 1 shows the variation in water production (WP) over time due to the addition of 1.0 wt% of nanoparticles, with $S_R = 0.5$ and $S_L = 0.2$. Note that this difference is maximum close to the breakthrough time and starts to decrease until it reaches zero. The right panel in Figure 1 presents the WP calculated at the breakthrough time for different initial and injection water saturation values. In this map, we observe two types of solution called CS- and SC-wave sequence; see [4] for details. Notice that, during water-gas co-injection within a certain parameter range, the addition of nanoparticles alters the mathematical solution, and in the entire region corresponding to the SC-wave sequence, nanoparticles do not affect water production.

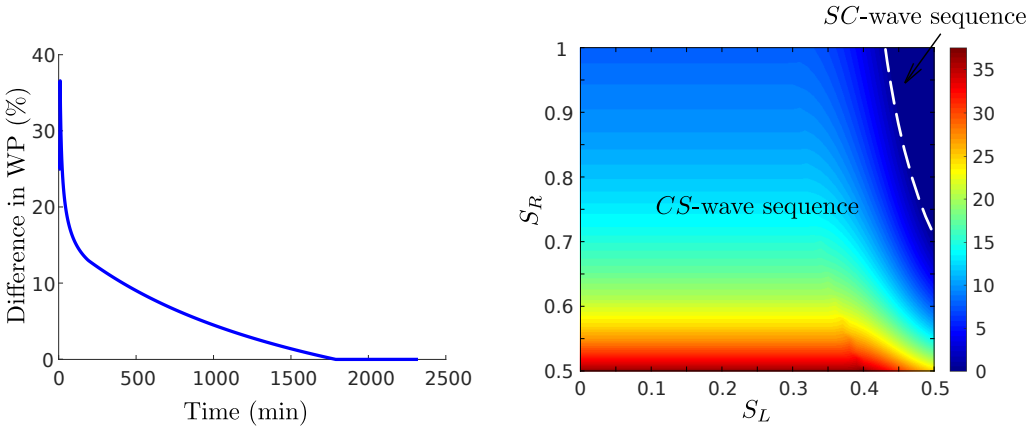

Figure 1: Mapping the difference in WP (%) due to the addition of 1.0 wt% of nanoparticles for $S_L \in [0, 0.5]$ and $S_R \in [0.5, 1]$ at the moment of breakthrough. The left panel shows an example of this difference over time for $S_R = 0.5$ and $S_L = 0.2$. Source: [2].

In [5], we performed uncertainty quantification and sensitivity analysis for NP-stabilized foam flow at local equilibrium, ignoring retention and using quadratic relative permeabilities. We inves-

tigated the breakthrough time (T_{bt}), WP, and pressure drop. The main result is that the effect of nanoparticles exceeds the model's uncertainty for all quantities, suggesting that it is statistically feasible to measure it in experiments. Figure 2 shows how uncertainty propagates for breakthrough time and WP. Note that nanoparticles reduce this uncertainty.

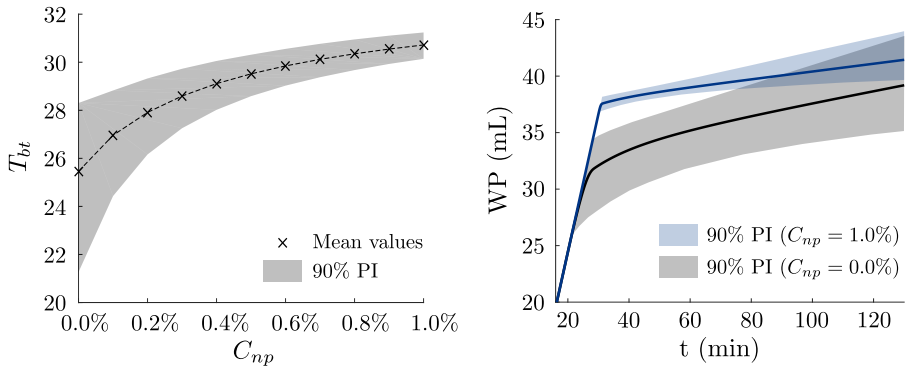

Figure 2: Uncertainty propagation for the breakthrough time and water production. Various concentrations are analyzed, from 0.0% (no nanoparticles) to 1.0% (max. nanoparticle concentration). Solid lines are the mean, while the shaded area indicates the 90% prediction interval. Source: [2].

3.2 Impact of Nanoparticles Retention on Pressure Drop

In [3], we investigated how nanoparticle retention affects the steady-state solution of system (2)-(6). The initial conditions corresponding to the water-saturated core with no bubbles or particles ($C = 0, \sigma = 0, n = 0, S_w = 1$) and the inlet boundary conditions corresponding to the co-injection of a chemical solution and gas ($C = C^I, P = P^I, n = 0.$). The retention constants λ and θ were obtained from [12] for four nanofluids: NF1 (0.1 wt% SiO_2), NF2 (0.1 wt% SiO_2 and 50000 ppm NaCl), NF3 (0.5 wt% SiO_2), and NF4 (0.5 wt% SiO_2 and 5000 ppm NaCl). Additionally, we have included two artificial nanofluids: NF5 (1.0 wt% SiO_2) and NF6 (1.0 wt% SiO_2 and 5000 ppm NaCl), as summarized in Table 2. We also adopted $\theta_g = 0.5\theta_w$ and $\Gamma = 0.3\lambda L$ [3].

Table 2: Nanoparticle retention parameters. Source: [12].

Nanofluid	λ (m^{-1})	θ_w (−)	Nanofluid	λ (m^{-1})	θ_w (−)
NF1	1.51	2013	NF4	5.33	913
NF2	2.95	3269	NF5	1.86	1312
NF3	1.86	1312	NF6	5.33	913

Without retention, nanoparticles improve sweep efficiency by increasing the foam's apparent viscosity, which lowers water saturation and increases pressure drop. Considering retention, the loss of suspended nanoparticles reduces their contribution to the foam's apparent viscosity, increasing water saturation and lowering pressure drop, while retained nanoparticles reduce permeability, leading to a higher pressure drop. Thus, the overall impact on pressure depends on which effect prevails. To analyze this, we compared total pressure drop without retention ($\Delta P_{\lambda=0}$), with retention but no permeability reduction ($\Delta P_{\theta_w=0}$), and with both factors (ΔP); see Fig. 3. Salt increases ionic strength and particle retention, making retention effects more significant. Our results

show that models neglecting retention and those considering retention but ignoring permeability reduction underestimate pressure drop. If the complete model is assumed to be more accurate, neglecting permeability reduction introduces more error than entirely ignoring retention effects.

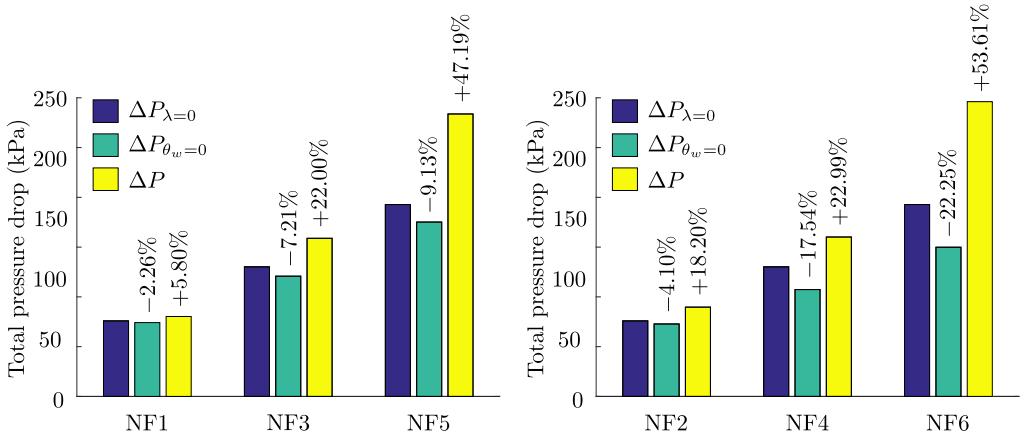

Figure 3: Total pressure drop for NP-stabilized foam flow at steady-state without (left panel) and with (right panel) NaCl. We study the pressure drop without particle retention ($\Delta P_{\lambda=0}$), with retention but no permeability reduction ($\Delta P_{\theta_w=0}$), and considering both effects (ΔP). The numbers on top of each bar indicate the pressure drop variation in relation to $\Delta P_{\lambda=0}$. Source: [2].

4 Conclusions

When comparing the two models presented in this work, the local equilibrium model, although simpler, provided valuable insights into breakthrough time, water production, and pressure drop over time, key quantities for industrial applications. On the other hand, the population balance model allowed us to examine the effects of particle retention on foam flow. However, its complexity required the analytical investigation to be conducted under steady-state conditions, limiting the analysis of dynamic parameters.

The results indicate that optimal conditions for maximizing water production in NP-stabilized foam core-flooding experiments occur in partially saturated cores (water saturation from 50 to 60%), with a co-injection water/gas ratio up to 40/60%. The uncertainty propagation study suggests that measuring nanoparticle effects is statistically feasible. Retention can decrease pressure due to suspended nanoparticle loss, but it may also increase pressure by reducing permeability. Considering both factors results in a greater pressure drop than models that ignore retention. In contrast, ignoring permeability reduction leads to a lower pressure drop.

Acknowledgments

The authors gratefully acknowledge support from Shell Brasil through the project “Avançando na modelagem matemática e computacional para apoiar a implementação da tecnologia ‘Foam-assisted WAG’ em reservatórios do Pré-sal” (ANP 23518-4) at UFJF and the strategic importance of the support given by ANP through the R&D levy regulation. G.C. was partly supported by CNPq grants 306970/2022-8, 405366/2021-3, and FAPEMIG grant APQ-00206-24.

References

[1] P. Bedrikovetsky, D. Marchesin, F. Shecaira, A. L. Souza, P. V. Milanez, and E. Rezende. "Characterisation of deep bed filtration system from laboratory pressure drop measurements". In: **J. Pet. Sci. Eng.** 32.2 (2001), pp. 167–177.

[2] T. Danelon. "Modeling nanoparticle-stabilized foam flow in porous media: Mathematical analysis and uncertainty quantification". PhD thesis. Federal University of Juiz de Fora, 2025.

[3] T. Danelon, R. Farajzadeh, P. Bedrikovetsky, and Grigori Chapiro. "Modeling nanoparticle-stabilized foam flow in porous media accounting for particle retention and permeability reduction". In: **Interpore J.** 2 (2025).

[4] T. Danelon, P. Paz, and G. Chapiro. "The mathematical model and analysis of the nanoparticle-stabilized foam displacement". In: **Appl. Math. Model.** 125 (2024), pp. 630–649.

[5] T. Danelon, B. M. Rocha, R. W. dos Santos, and G. Chapiro. "Sensitivity analysis and uncertainty quantification based on the analytical solution for nanoparticle-stabilized foam flow in porous media". In: **Geoenergy Sci. Eng.** 242 (2024), p. 213285.

[6] D. Du, D. Zhao, F. Wang Y. Li, and J. Li. "Parameter calibration of the stochastic bubble population balance model for predicting NP-stabilized foam flow characteristics in porous media". In: **Colloids Surf. A Physicochem. Eng. Asp.** 614 (2021), p. 126180.

[7] Ø. Eide, M. Fernø, S. Bryant, A. Kovscek, and J. Gauteplass. "Population-balance modeling of CO_2 foam for CCUS using nanoparticles". In: **J. Nat. Gas Sci. Eng.** 80 (2020), p. 103378.

[8] R. Farajzadeh, P. Bedrikovetsky, M. Lotfollahi, and L. W. Lake. "Simultaneous sorption and mechanical entrapment during polymer flow through porous media". In: **Water Resour. Res.** 52.3 (2016), pp. 2279–2298.

[9] J. M. A. Godoi and P. H. L. S. Matai. "Enhanced oil recovery with carbon dioxide geosequestration: First steps at pre-salt in Brazil". In: **J. Pet. Explor. Prod. Technol.** 11 (2021), pp. 1429–1441.

[10] J. P. Herzig, D. M. Leclerc, and P. Le. Goff. "Flow of Suspensions through Porous Media—Application to Deep Filtration". In: **Ind. Eng. Chem. Res.** 62.5 (1970), pp. 8–35.

[11] G. J. Hirasaki and J. B. Lawson. "Mechanisms of Foam Flow in Porous Media: Apparent Viscosity in Smooth Capillaries". In: **SPE J.** 25.02 (1985), pp. 176–190.

[12] A. Keykhosravi, P. Bedrikovetsky, and M. Simjoo. "Experimental insight into the silica nanoparticle transport in dolomite rocks: Spotlight on DLVO theory and permeability impairment". In: **J. Pet. Sci. Eng.** 209 (2022), p. 109830.

[13] Q. Li and V. Prigiobbe. "Modeling Nanoparticle Transport in Porous Media in the Presence of a Foam". In: **Transp. Porous Media** 131.1 (2020), pp. 269–288.

[14] M. Simjoo, Y. Dong, A. Andrianov, M. Talanana, and P. L. J. Zitha. "Novel Insight into Foam Mobility Control". In: **SPE J.** 18.3 (2013).

[15] B. Sudret. "Meta-models for structural reliability and uncertainty quantification". In: **APSSRA**. Singapore: HAL, 2012, pp. 1–24.

[16] N. Yekeen, M. A. Manan, A. K. Idris, E. Padmanabhan, R. Junin, A. M. Samin, A. O. Gbadamosi, and I. Oguamah. "A comprehensive review of experimental studies of nanoparticles-stabilized foam for enhanced oil recovery". In: **J. Pet. Sci. Eng.** 164 (2018), pp. 43–74.

[17] P. L. J. Zitha and D. X. Du. "A New Stochastic Bubble Population Model for Foam Flow in Porous Media". In: **Transp. Porous Media** 83.3 (2010), pp. 603–621.

